2007

Electrospun Blends of Polydioxanone and Fibrinogen for Urological Applications

Joshua Ford Grant
Virginia Commonwealth University

ELECTROSPUN BLENDS OF POLYDIOXANONE AND FIBRINOGEN FOR UROLOGICAL APPLICATIONS

A Thesis submitted in partial fulfillment of the requirements for the degree of Masters of Science in Physiology at Virginia Commonwealth University.

by

JOSHUA GRANT
B.A., Goucher College, 2001

Director: GARY L. BOWLIN, PH.D.
ASSOCIATE PROFFESOR, BIOMEDICAL ENGINEERING

Virginia Commonwealth University
Richmond, Virginia
May, 2007

Acknowledgement

First and foremost, would like to thank Dr. Gary Bowlin for allowing me the privilege of working in your lab. Your friendship and guidance will be much missed next year. I know despite our different tastes in backpack aesthetics, we can always agree on lunch. I would like to thank Catherine Barnes, Scott Sell, Michael McClure, and Mathew Smith. Your help and guidance prevented me from incurring serious bodily injury. Dr. Simpson, your help with all things histology was much appreciated. I would like to thank Dr. George Ford, for sitting on my committee, and guiding me these past two years. Finally, I would like to thank my parents, Mel and Wendy Grant, and my brother, Jeremy Grant, for always supporting me.

Table of Contents

List of Tables

Page

List of Figures

Page

Abstract

ELECTROSPUN BLENDS OF POLYDIOXANONE AND FIBRINOGEN FOR UROLOGICAL APPLICATIONS

By Joshua Ford Grant, B.A.

A Thesis submitted in partial fulfillment of the requirements for the degree of Masters of Science in Physiology at Virginia Commonwealth University.

Virginia Commonwealth University, 2007

Major Director: Dr. Gary L. Bowlin
ASSOCIATE PROFFESOR, BIOMEDICAL ENGINEERING

The need for tissue and organ replacements cannot be satisfied by autograft and allografts alone. The purpose of this study was to investigate the feasibility of electrospinning a blend of polydioxanone and fibrinogen to produce an engineered tissue scaffold. Fiber diameter and pore size of blends were characterized, as well as mechanical strength. Cell proliferation assays for 1 and 7 day cultures were preformed, and a histological evaluation was performed to determine how favorable the various blends were to cell infiltration and proliferation. Some ratios of blends were identified that contained

both acceptable mechanical properties and properties that facilitated cell infiltration. These findings pave the way for future refinement and use of these scaffolds for a variety of tissue engineered targets.

Introduction

Background

Biomedical engineering represents the convergence of multiple disciplines of science. This convergence of disciplines allows complex issues in health care to be addressed. One rapidly expanding area of biomedical research is tissue engineering. Tissue engineering aims to replace and repair damaged or diseased tissues and organs. The demand for replacement organs is daunting. It is estimated that treatment for patients with organ failure exceeds $400 billion dollars a year [1]. While the nation's organ transplant centers are able to supply some allographic tissue and organs, the demand and waitlist for these organs is increasing [2]. Tissue engineering research offers promise to alleviate this demand for allographic tissue. Research into replacing organs is ongoing**.** Despite successes in the field such as dermal tissue engineering [3], many other organ systems are awaiting a successful replacement. One such system that would greatly benefit from the advent of non-autologous, off the shelf tissue is the urinary system.

Urinary System Overview

The urinary system plays a vital role in the body. In addition to its obvious function in the removal of metabolites via excretion, it plays a pivotal role maintaining homeostasis. The urinary system is responsible for maintenance of salts, acids and bases, and secretion

of hormones. The urinary system is composed of four major components; the kidney, the ureters, the bladder, and the urethra.

Removal of nitrogen is an important function of the kidneys. Amino acid catabolism occurs in the liver. Nitrogen from amino acids is converted to urea, and enters the blood stream. Urea is then removed from the blood by the kidneys. The kidneys also aid in maintaining the balance of important ions including potassium, bicarbonate, calcium ions, as well as function in the regulation of blood pH through a process of absorption and secretion. The filtrate filtered by each kidney is then passed to the ureters, which serve to deliver urine to the bladder. Delivery is aided by peristalsis. Ureters consist of the inner mucosal layer, followed by a layer of smooth muscle cells. The urethra connects the bladder to the exterior of the body, allowing urine to be excreted [4].

The integrity of the urethral and urethral conduits are vital for the preservation of renal function, and thus homeostasis. Typically, surgical procedures involving reconstruction of the ureter arise from urinary tract obstructions, carcinoma, or trauma sustained from injury. Left untreated, these maladies can give rise to symptoms ranging from patient discomfort, to renal failure and death. Likewise, problems with the urethra can also negatively impact quality of life. Urethra corrected with reconstruction include hypodispias, stricture, and tumor growth. Treatments for these diseases have inherent problems, and more solutions should be pursued in order to further patient care.

Urinary Tract Disorders

Urinary tract obstruction (UTO) is one of several disorders associated with the urinary tract. It has also been reported that 166 out of 100,000 hospital visits in the United

States were a result of UTO [5]. Clinical presentation of the disease depends on the severity of the obstruction. If a single ureter is obstructed (unilateral obstruction), a patient may present with dull flanking pain, but might also be asymptomatic. Bilateral obstruction however, is accompanied by either lower abdominal or back pain, and may progressively show symptoms of renal failure. In such cases, the renal pelvis becomes dilated and enlargement of the kidney occurs resulting in hydronephrosis.

In a series of over 32,000 autopsies, it was found that 3.8% had hydronephrosis, dilation of the renal pelvis due to UTO [5]. Typically hydronephrosis is associated with atrophy of the renal parenchyma**.** Three mechanisms associated with hydronephrosis lead to renal failure: pressure atrophy, intrarenal reflux, and ischemia. Pressure atrophy is associated with an increased pressure in the renal pelvis. Pressure results in the atrophy of the renal medulla leading to renal failure. In this case, renal papillae are distorted, leading to decreased sodium, potassium, and water handling in the distal tubular and collecting ducts. Intrarenal reflux occurs when urine moves retrograde to the kidneys. It results in cortical and medullary atrophy. Ischemia is associated with the obstruction and occlusion of local vasculature around the renal pelvis associated with enlargement of the renal pelvis. It is this decrease in blood flow that ultimately leads to ischemic atrophy in the kidney. Hydronephrosis is of great concern when dealing with UTO due to these three mechanisms leading to organ failure. The disease is treated surgically with an ileal conduit, although complications do occur [6, 7].

Hypertension is also a complication associated with UTO. Resulting fluid retention due to UTO causes extracellular matrix expansion. Renin is a soluble plasma enzyme

responsible for elevating blood pressure by activating angiotensin. Elevated renin levels are associated with UTO, and explain hypertension. It has been observed however that removal of the obstruction helps to rectify elevated renin and diminishes hypertension [8].

Tumors can also induce obstruction and stricture of both the ureter and urethra. Transitional cell epithelium lines the lumen of the urinary tract. Roughly 90% of carcinomas develop in the bladder and the proximal two thirds of the urethra. Tumors in the ureter account for only 2% of carcinomas in the UT. Tumors of the urinary tract are polychronotropic, meaning, that they can reappear over both time and space. In fact, an estimated 50%- 70 % of patients with a tumor located in the mucosa will have a recurrence. Typical management for urinary tract tumor is resection. Recurring tumors require additional resection, decreasing the amount of urinary tract tissue [9].

Proper recognition and treatment of UTO is clearly important. Although proper treatments include placement of a bladder catheter, nephrostomy, pyelostomy, cutaneous ureterostomy, suprapubic cystostomy, or ileal conduit; each is accompanied by risks of recurrent obstruction, ascending urinary tract infection, electrolyte abnormalities, volume depletion, and formation of renal calculi. Although these treatments are effective in some cases, better treatments should be pursued.

Urethral defects and maladies negatively impact the quality of life of many patients. Two problems of the urethra are hypospadias and urethral strictures. Hypospadias is a congenital defect where there is incomplete development of the urethra. The urethral opening subsequently appears anywhere on the ventral side of the penis, the scrotum, or perineum. Upwards of 1 in 150 births are diagnosed with hypospadias [10]. Typically,

early surgery is used to correct this defect [11]. In severe cases, autologous tissue from nonpenile skin, bladder, or buccal mucosa is used to repair urethral defects [12].

Urethral strictures are typically caused by traumatic injury and inflammation. Patients with strictures typically present with trouble voiding. Although treatment such as stents are a nonsurgical option [13], reconstructive surgery is employed for more severe cases. Grafts from other donor sites, such as penile skin [14], small intestine submucosa [15], and buccal mucosa [16], can also be used for the more complex repairs. Despite continually advancing surgical procedures, the instance of complications for repair is 30% [10].

In regards to the ureters, obstruction can manifest itself through a range of symptoms, from patient discomfort to renal failure. Obstruction of the ureter due to strictures has been treated in the past surgically with varying degrees of success. Typically, problems arise when patients have a pre-existing condition with colonic or ileum tissue, or via metabolic problems incurred by removal of gastrointestinal tract [17, 18]. Metabolic acidosis, vitamin B-12 deficiency, and chologenic diarrhea have all been noted as problems associated with the use of colonic segments as a ureter substitute [19]. In general, use of a tissue autograft in urinary tract reconstruction is associated with inadequate biocompatibility, lack of peristaltic activity, and build up of salt deposits [1]. In addition, an autograft may cause prolonged surgical time, extended hospitalization, and an increase in morbidity. [20]

Although bowel segments have been shown effective in some cases, new alternatives are actively being pursued. One recent alternative is a self expanding,

intraluminal metallic stent. [21] These stents have shown to be effective in some animal models, but also have inherent problems. Problems with these stents include hydroureteronephrosis, severe urothelial hyperplasia, stent migration, stone formation, and infection. Recent stent enhancements include lining metal stents with polycarbonate [22]. These stents were shown to reduce hydroureteronephrosis in a canine model, but were still not a total solution to obstruction.

Urological disorders are both problematic to treat and degrade quality of life. As described above, multiple UT maladies are treated by surgical intervention. Tissue engineering presents itself as a promising field in the treatment of urological disorders. Native local urological tissue is often the source of tissue for reconstruction, but often this option is not feasible. Investigation into novel materials and techniques has been suggested for developing materials that can be used as a substitute for natural tissue.

Review of Engineered Urological Tissue

Natural materials have been considered for engineered urological tissues. Acellular collagen matrix obtained from porcine bladders was investigated as a urethral replacement. In an early study, an acellular tubular collagen sponge proved successful in regenerating uro-epithelail cells along the inner wall when implanted in dogs. These scaffolds importantly did not illicit hydronephrosis [23]. Further studies with collagen sponges showed that these scaffolds were seen to preserve urethra morphology, promote migration of host cells, and induce angiogenesis into the graft itself [20]. It was later noted that uroepithelial cells cultured on meshes of poly(glycolic acid) and implanted into rats and

rabbits formed multiple layers of cell lining [24]. Despite this initial success in experiments involving ureters, more recent studies in a canine model did not prove as promising [25]. Despite the current attempts at engineered materials, there is no tissue engineered effective treatment for urological strictures of the ureter.

Tissue Engineering

Many routes of tissue fabrication have been pursued. Some have proven effective, other methods have not. Fundamentally, tissue engineering involves deposition of cells onto a scaffold, or matrix. Much consideration has been given to the ideal scaffold. Macroscopic properties such as strength and modulus can affect the usefulness of the scaffold just as much as microscopic properties such pore size and fiber diameter. Bioactivity, environments which promote cell attachment and proliferation is also paramount [26]. The past several decades has seen many materials used, however none has proven totally effective in matching tissue specific matrices [27].

Tissue engineering is a rapidly expanding, dynamic field of study. Specifically, tissue engineering strives to develop novel replacements for biological tissue. Cells, extracellular matrix (ECM), and signaling systems are all vital for a functioning tissue. Our laboratory is concerned with recreating ECM with both natural and synthetic proteins. In tissues, the ECM contains collagen, glycosaminoglycans, hyaluronic acid, proteoglycans, and elastins. In addition to these constituents, enzymes that degrade the matrix and their inhibitors are present, allowing for dynamic remodeling of the ECM [28].

Cells interact with the ECM via specialized cell receptors. Integrins, transmembrane proteins composed of heterodimeric α and β subunits, play a vital role in

interactions between the cell and extracellular matrix. Upon binding a ligand, integrins illicit a response through the cytoskeleton and cytoplasmic kinases [29]. Signaling cascades can modify many cellular characteristics such as morphology, proliferation, and genetic regulation.

Typical engineered scaffolds are made of either natural polymer or synthetic polymer. Poly(glycolic acid) (PGA), poly(lactic acid) (PLA) and polycaprolactone (PCL) have all seen extensive use in tissue engineering. [1] Natural polymers use has included collagen , elastin, fibrinogen, hemoglobin, and myoglobin.

In addition to material, scaffold architecture is an important consideration for tissue engineering. Fiber size should be around 50 to 500nm in diameter to mimic the ECM [30]. Pore size is an important characteristic of scaffolds. Macropores (>50nm , <300um) facilitate cell and tissue penetration where micropores (<2nm) and mesopores (>2nm , <50nm) allow for solute diffusion [31]. A study comparing cell infiltration into separate scaffolds containing electrospun type I collagen and gelatin respectively indicated lack of infiltration into gelatin, yet infiltration into collagen matrices. It was suggested that the smaller average pore size of gelatin (1500-4000 nm^2) precluded cell infiltration, while the pore size of collagen (2000-6000 nm^2) facilitated cell infiltration [32].

Electrospinning

Electrospinning of materials is one method by which the structure of the ECM can be reproduced. Although electrospinning is not a new technique, its applications to biomedical engineering are obvious. The physical basis of electrospinning revolves around two main principles, separation of charge and surface tension. In the 1880s, Lord

Rayleigh began investigating the properties that distort a water droplet. He noticed that as the electrical potential of the water droplet is increased, the droplet will begin to deform. Rayliegh determined that the stabilizing force, surface tension (T) was related to the charge Q by spherical radius a.

$$T > Q^2 / 16\pi a^3$$

An increasing charge will ultimately overcome the surface tension of the droplet, at which point liquid is thrown off in fine jets [33] .

A typical electrospinning setup is shown below. As the syringe (polymer reservoir) is depressed, a droplet of liquid forms on the tip of the syringe. This droplet is exposed to an electric field applied by a high voltage power supply. As the surface tension is overcome by the electrical field, liquid jets are accelerated towards an area of lower potential. Typically this area of lower potential is a grounded collection target.

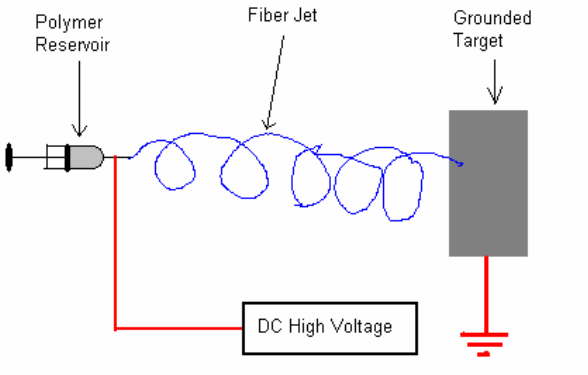

Figure 1. A schematic representation of an electrospinning setup. A high voltage power supply, solution reservoir, and grounded target are the major components of such a setup.

Although this system does not seem complex, many variables can be altered yielding with dramatically different results. Altering the potential, polymer, polymer concentration, solvent, and mandrel distance to target all yield dramatically different results [34, 35]. In addition, mechanical manipulation of the target can dramatically change the way in which the fiber is collected. By varying the parameters above, radically different results can be achieved. By finding the right combination of variables, a more viable tissue scaffold can be forged.

Polydioxanone

Polydioxanone (PDO) is a polymer that has been used extensively in biomedical applications, specifically in use as sutures. PDO is produced by ring opening of p-dioxanone monomers to form polydioxanone polymer. This process requires heat, and an organometallic catalyst such as zirconium acetylacetone, diethylzinc, or zinc L-lactate (ZnLac2) , and forms ether-ester bonds [36]. Low temperature however, should be used in order to prevent depolymerization to p-dioxanone during polymerization.

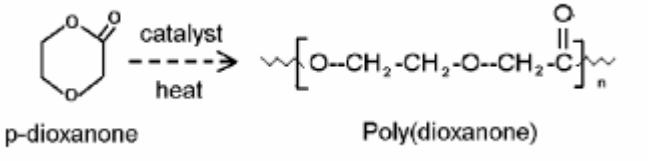

Figure 2: Polymerization of p-dioanone to polydioxanone [37].

PDO is typically extruded as a monofilament for suture use. The ether group along the backbone of PDO allows for its large degree of flexibility. PDO is biodegradable, but its degradation rate is much slower than other monofibers [38]. In addition, PDO exhibits a low inflammatory response compared to other polymers used in sutures [39]. Despite its potential benefits for use as a suture material, PDO has shape memory, which is a major drawback in use of sutures. While shape memory is a drawback for PDO in suture use, it may prove useful in maintaining structure of a tissue scaffold.

Although it has had limited use in other biomedical areas [40, 41], it has recently been proposed as an ideal material for tissue engineering. In fact, recent studies have suggested electrospun PDO might provide an ideal construct for a tissue scaffold [37]. Polydioxanone has a proven track record. Its use as a suture material has shown that it is biocompatible, and will illicit only a mild immune response. Further, PDO degrades by hydrolysis. Presumably, if used as a component of a tissue scaffold, PDO degradation might allow further cell infiltration and remodeling of the scaffold. It has been shown to be electrospun, producing fibers in the micron and submicron diameter. Such characteristics make it a suitable candidate for scaffold material.

Fibrinogen

Fibrinogen is a vital plasma protein involved in the coagulation cascade and wound healing. Fibrinogen is composed of six chains, chains two α, two β, and two γ chains linked by 29 disulfide bonds [42]. Vascular injury initiates a cascade that converts fibrinogen to fibrin via thrombin, a serine protease. The N terminal of fibrinogen alpha and beta chains

are cleaved, removing glutamate and aspartate residues. Negatively charged glutamate and aspartate residues prevent fibrinogen from aggregating until cleavage occurs. Upon cleavage, fibrin self assembles and forms fibrous clots, natural scaffolds where platelet aggregation occurs.

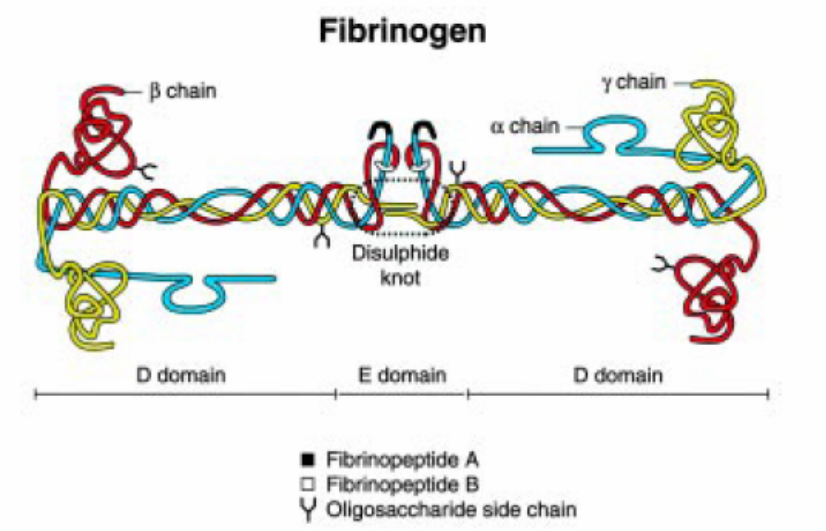

Figure 3: The structure of fibrinogen. [42]

Upon injury to a blood vessel, collagen and subendothelial matrix-bound vWF are exposed. Platelets, non-nucleated cells that assist in occluding vascular injuries, contain glycoproteins on their plasma membranes that have affinity for collagen and subendothelial matrix-bound vWF. In particular, collagen binding to GPIa glycoprotein on platelets causes morphological changes in platelets. These morphological changes induce platelets to become spherical, extend pseudopods, and increase platelet-platelet interactions. In addition, GPIa binding causes conformational changes to occur in GPIIb/IIIa, glycoproteins on the platelet plasma membrane. This glycoprotein binds vWF and fibrinogen. As platelets aggregate, they degranualize. An important component of the

platelet granules is adenosine diphosphate (ADP). ADP causes conformational changes which allow for increased GPIIb/IIIa binding.

Two thrombin activating pathways exist, the intrinsic and extrinsic pathway. The extrinsic pathway is initiated by external stimuli such as blunt trauma, while the instrinic pathway is initiated by internal stimuli. Both stimuli activate proteases that ultimately activate thrombin. Sequential activation of the cascade allows for amplification of the signal. Factor XIII is activated during the clotting cascade, this factor serves to crosslink glutamine and lysine residues on fibrin [43, 44].

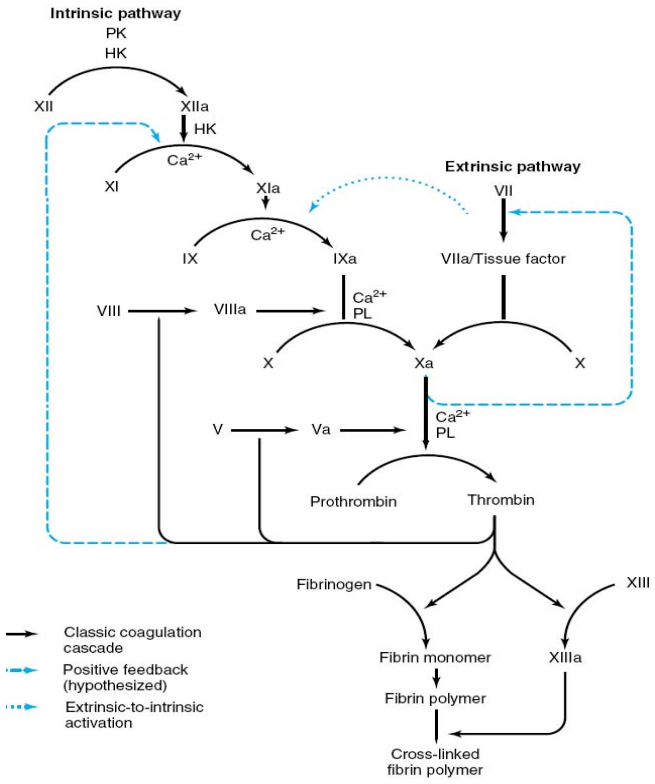

Figure 4: Illustration of the coagulation cascades catalyzing the formation of cross linked fibrin polymers from fibrinogen [45].

Fibrin serves as a natural scaffold in the event of traumatic injuries. Fibrin's inherent bioactivity allows it to act as a surrogate scaffold after it is assembled into a clot. Two characteristics allow fibrin to achieve its goal. First, the polymerization forms a clot, giving a physical framework, or scaffold for the invasion and proliferation of cells. Second, fibrin contains bioactive domains that allow the attraction of cells. These domains include integrin binding domains which are attachment points for cells.

Both the structural characteristics and domains that signal cells allow fibrin to be bioactive. It is vital that the scaffolds contain these bioactive domains, but also that the scaffolds themselves do not impede migration of cells to these domains. After conversion of fibrinogen to fibrin, exposure of receptor binding sites elicit specific fibrin dependant cell responses.

Bioactivity of Fibrinogen

One way in which cells interact in their environment is integrin receptors. Integrins are an integral membrane protein that spans the plasma membrane. Integin is responsible for binding to ligands on either other cells or the extracellular matrix. Fibrinogen and fibrin contains three integrin binding sites. These binding sites, or ligands, include two RGD sequences on the alpha chain (RGDS α572+/-575 and RGDF α95+/-98) and a non RGD sequence on the gamma chain (carboxy terminal γ400+/-411) [42]. These sequences are made up of arginine, glycine, and aspartic acid amino acids. Both fibrinogen and fibrin also act through non-integrin receptors [46]. Fibrin can act through ICAM-1 (Intercellular Cell Adhesion Molecule) dependant pathways, promoting intercellular adhesion by acting as a bridge.

Fibrin and fibrinogen cleavage products also act as mitogens, inducing mitosis in endothelial cells, fibroblasts, mesotheilial cells, smooth muscle cells and lymphocytes. Fibrinopeptide B cleaveage and the exposure of the amino terminus of the fibrin β chain enhance fibroblast and endothelial cell proliferation. This has been a suggested pathway for the enhanced proliferation of fibroblasts and endotheial cells in response to injury [47]. Intact fibrinogen is mitogenic for lymphoid cells and hemopoietic progenitors. The mitogenic effect here is mediated by two non-integrin binding sites, a 92+/-94 kDA mitogenic fibrinogen receptor (MFR) and a ICAM-1 site. Downregulation of MFR may explain why normal cells do not proliferate in the circulation [48]. Fibropeptide fragments α and β, in addition to fibrinogen products produced during cleavage by thrombin have been shown to have proliferatory effects on fibroblasts [49].

Fibrin matrices also elicit migratory effects on certain cells including endothelial cells, fibroblasts, macrophages, smooth muscle cells, keratinocytes and tumor cells. Fibrinogen cleavage products have been shown to act as chemoatractants for neutrophils, monocytes and fibroblasts. Specific chemoattractants include fibrinopeptide B (Bβ1+/-14) when released from fibrinogen by thrombin, and fibrinogen peptide (Bβ1+/-42). These two chemoatractants act comparatively to leukotriene B_4 and platelet derived growth factor (PDGF) respectively [50].

Due to its inherent bioactivity, fibrinogen has been examined by tissue engineers in the past. Fibrinogen has been wet extruded with fibronectin into cables for use as a tissue scaffold, producing fibers 0.5mm in diameter [51]. Fibrinogen has been studied as a scaffold for chondrocytes in order to mimic cartilage [52, 53]. Fibronectin scaffolds doped

with fibrinogen have been shown to illicit a greater amount of cell migration compared to fibronectin scaffolds alone [54]. It is clear that fibrinogen certainly exhibits advantageous bioactivity in vitro.

Further refinement of engineered fibrinogen constructs might offer a suitable scaffold for a variety of uses. Problems with several of the above applications of fibrinogen include large fiber size, and diminished structural strength when compared to many synthetic polymers. It has been reported that polyethelene glycol (PEG), a synthetic polymer, was modified with fibrinogen and used as scaffolds with a large degree of success. This scaffold makes use of PEG molecules bound to a fibrinogen backbone so that the scaffolds retain the bioactivity of fibrinogen, yet also retain the mechanical properties, and cellular transparency of PEG. The use of a synthetic polymer and a natural polymer present an ideal solution for engineering a scaffold that is both bioactivley and mechanically sufficient respectively [55].

Electrospinning has shown its ability to produce nanoscale, biocompatible fibers in the past [56, 57]. Fibrinogen for example has been successfully electrospun and characterized [58, 59]. Electrospun fibrinogen has very poor mechanical characteristics, especially when hydrated. It was suggested that mechanical properties of hydrated fibrinogen could be improved by chemical crosslinking of fibers. Glutaraldehyde exposure, a crosslinker that cross links R-group amines of lysine residues to amino groups on other amino acids [60], was shown in vitro to have a negligible effect on mechanical properties of electrospun scaffolds [59]. Although electrospun fibrinogen offers benefits compared to extruded fibrinogen fibers and hydrogels, its mechanical properties fall short of ideal. In

order to make use of fibrinogen as a scaffold, its mechanical properties need to be improved.

Goals

The goal of this research was to take two previously electrospun and characterized polymers and blend them, combining characteristics of both. Specifically, blended products should contain both the mechanical strength of polydioxanone, and the bioactivity of fibrinogen, in addition retaining fiber diameters and pore sizes that are similar to those of the ECM.

Materials and Methods

Solution Preparation

A stock solution of 120 mg/ml Fibrinogen (Sigma-Aldrich Chemical Company) was dissolved in HFP (in 9 parts 1,1,1,3,3,3-hexaflouropropanol (HFP; Sigma-Aldrich Chemical Company) and 1 part 10x minimal essential media and sodium bicarbonate) at a concentration of 0.083 g/mL was made**.** Polydioxanone stock solution was created by dissolving 100 mg/ml PDO (Ethicon) in HFP. Since mixing the two solutions causes fibrinogen to precipitate, a novel coaxial electrospinning (Appendix 1) setup was used. The coaxial nozzle was set up so that PDO solution exited the core of the tip, while fibrinogen exited around the core. For each sample different ratios of PDO and FBG were used, but were kept in separate syringes to prevent precipitation, 4 mL of total solution was electrospun. Each 4 ml sample differed by 10% volume of PDO and Fibrinogen (FBG). Samples included both pure PDO and pure fibrinogen, for a total of eleven samples. Solutions were loaded by volume into separate Becton Dickinson syringes (3 ml or 5 ml). A table of volumes is shown below.

Ratio PDO:FBG	Volume PDO (mL)	Volume FBG (mL)
100:0	4.0	0.0
90:10	3.6	0.4
80:20	3.2	0.8
70:30	2.8	1.2
60:40	2.4	1.6
50:50	2.0	2.0
40:60	1.6	2.4
30:70	1.2	2.8
20:80	0.8	3.2
10:90	0.4	3.6
0:100	0.0	4.0

Table 1: Volumes of PDO and FBG used for each scaffold produced.

Electrospinning

In order to maintain a total overall solution deposition rate across samples, two separate KD Scientific syringe pumps were used. Using two pumps (KD Scientific Model 100) allow for conservation of the overall solution deposition rate of 4 ml/hr. An 18-gauge blunt needle was attached to the syringe. Tygon tubing with a 0.050" inner diameter and a 0.090" outer diameter was placed over each blunt needle, and attached to the coaxial nozzle. The syringe containing fibrinogen was connected to the outer coaxial layer, while the polydioxanone was attached to the inner coaxial layer. The nozzle itself was positioned on top of a stand and connected to the positive lead of a high voltage supply (Spellman CZE1000R; Spellman High Voltage Electronics Corp.). A stainless steel, grounded target

(2.5 cm wide × 10.2 cm long × 0.3 cm thick) was rotating between 500 and 1000 revolutions per minute (RPMs), and placed 15 cm from the nozzle.

Uniaxial Tensile Testing.

Tensile testing was performed to failure on both dry and hydrated samples (soaked in phosphate buffered saline (PBS) for 24 h). Samples were cut from an electrospun mat using a 'dog-bone' shaped punch (2.75 mm wide at its most narrow point and gage length of 7.5 mm). Thickness of samples were recorded, and samples were tested using a MTS Bionix 200 with a 50 N load cell (MTS Systems Corp.). An extension rate of 10.0 mm/min was used. MTS software Testworks 4.0 was used to calculate and record elastic modulus, peak stress, and strain at failure.

Scaffold Characterization

Samples from each scaffold were taken and sputter coated in gold (Electron Microscope Sciences model 550) for scanning electron microscopy (Zeiss EVO 50 Scanning Electron Microscope, SEM). Images at 2000x were taken and analyzed by ImageTool 3.0 **(**Universiry of Texas Science Center in San Antonio, Shareware**)** in order to determine average fiber diameter and pore area. Calibration was performed using the scale bar on each SEM. Averages were determined by taking 60 measurements of both fiber diameter and pore area for each sample.

Fibroblast Cell Culture

In order to determine cell proliferation, human dermal fibroblasts (HDF, ATCC CRL-2522) were cultured using 20 mL 1:1 DMEM/F12 (Gibco), 10 % heat inactivated Fetal Bovine Serum **(**Mediatech), 1% Pennacilin-Steptomycin (10,000 units/mL Penecylin G, 10,000 µg/mL Streptomycin, Gibco) media in 150 cm^2 sterile tissue flasks. Cultures were stored in a 37°C humidified CO_2 incubator and media refreshed every 2 days. Cells were subcultured in a ration of 1:3 using 0.25% Trypsin-EDTA (Gibco). This study used cells from passages 4-5.

Scaffold Preparation

Scaffolds were disinfected by soaking in ethanol for 10 minutes, followed by four successive 10 minute soaks in 1x Dubecco's Phosphate Buffered Saline (MP Biomedicals). While still in PBS, scaffolds were punched with 10 mm^2 biopsy punches (Picu Punch, Acuderm) and placed in 48 well cell culture cluster plates (Corning). Pyrex 10x10mm cloning rings (Corning) were then placed on top of the scaffolds to fix the position of the scaffold. 200 µl of PBS was added into the cloning ring, and the plates were incubated overnight in a 37°C humidified CO_2 incubator. PBS was removed immediately prior to seeding.

Cell Seeding

HDFs were seeded 10,000 cells/well in an initial volume of 50 µl of supplemented DMEM/F12 on PDO-Fibrinogen scaffolds (n = 5). After 45 minutes, an additional volume

of 150 µl was added, for a total of 200 µl. Cells were incubated on the scaffold for one and seven day periods. The media in the seven day culture was changed every two days.

Cell Proliferation Assay

In order to determine cell proliferation, a colorimetric MTS assay was used (Chemicon). In this assay, MTS reagent WST-1 (3-[4,5-dimethylthiazol-2-yl]-5-[3-carboxymethoxyphenyl]-2-[4-sulfophenyl]-2H-tetrazolium) reacts with mitochondrial cytochrome C in order to produce soluble formazan dye. The concentration of dye in solution can be quantified by measuring the absorbance at 420-480 nm. Scaffolds were removed from their incubation wells and placed in fresh wells. 200 µl of fresh media was added and 20 µl MTS assay was added to each well. Plates were incubated for two hours. After incubation, plates were shaken on a Fisher Vortex Genie II shaker for one minute. Aliquots from each scaffold were taken and pipetted into a 96-well plate. The absorbance was measured at 450nm on a Molecular Devices SpectraMAX^{384} spectrophotometer.

Histology

Hematoxylin and Eosin (H&E) staining on 1 and 7 day culutres was preformed by Harris Histology Inc, Greenville NC. Micrographs of sections were taken with a Nikon Eclipse TE300 light microscope at 20x magnification.

Statistics

All statistical analysis was performed using a one-way analysis of variance and Tukey-Kramer pairwise multiple comparison procedure ($\alpha = 0.05$). Analysis was performed using JMP®IN 4.03, statistical software (SAS Institute, Inc.).

Results

Fiber Diameter and Pore Size

SEM of different ratio dry scaffolds were taken at 2000x (Figure 5) and used to determine fiber diameter and pore size (Figure 6 and 7, respectively) Fiber diameter ranged from a minimum of 0.3±0.1 μm in 0:100 samples to 1.7±0.6 μm in 100:0 samples. Average fiber diameter was seen to increase as the content of PDO increased. Fiber diameter of samples with higher PDO concentrations were significantly different than those with lower concentration.

Pore size is shown to range from minimum 6.5±2.0 μm in 30:70 samples to 14.0±2.0 μm in 100:0 samples. Pore size was shown to be statistically different in several samples. In general scaffolds containing higher concentrations of PDO were different than scaffolds containing lower concentrations of PDO. Samples with higher concentrations of PDO tended to have larger pore sizes.

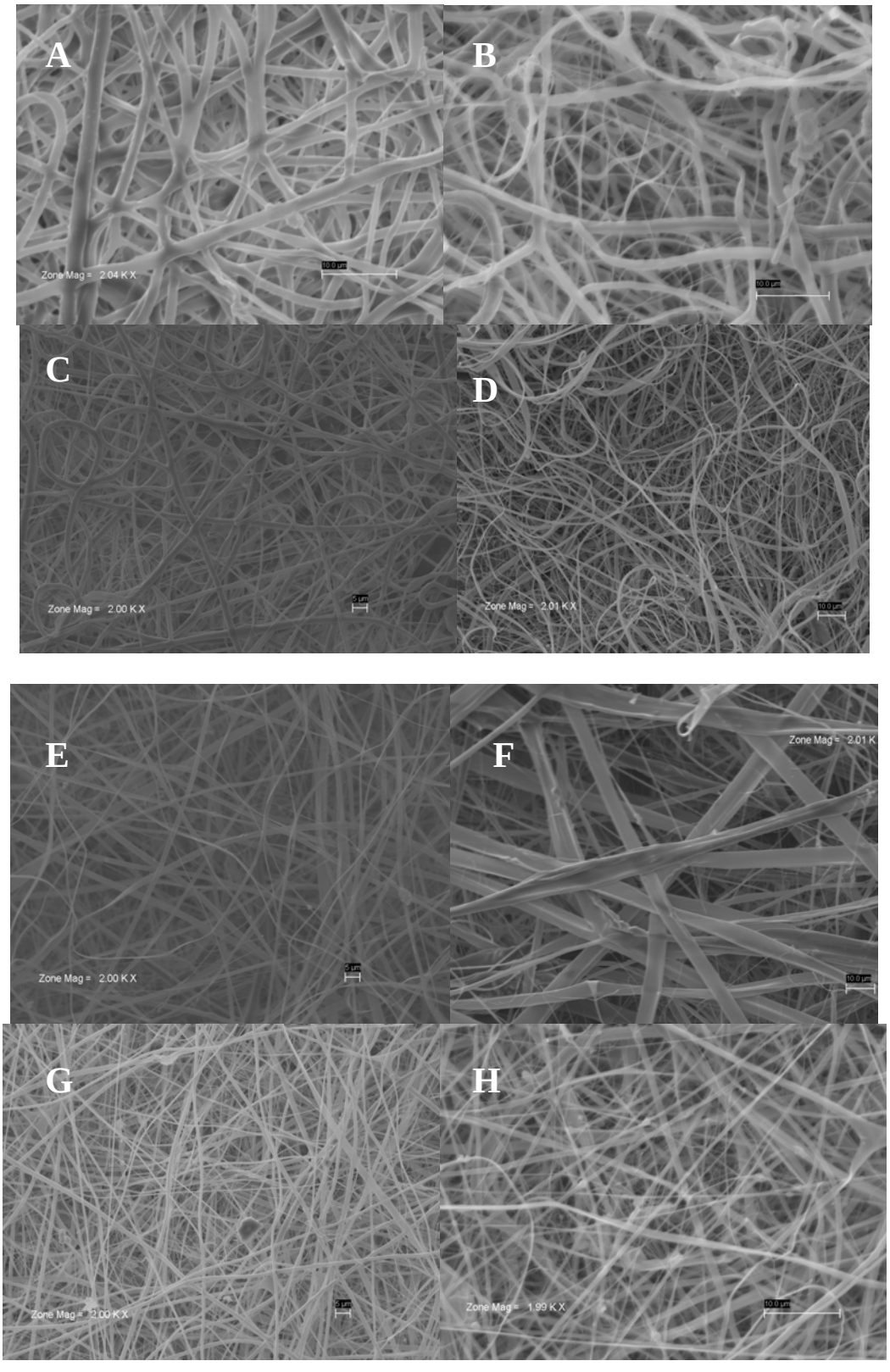

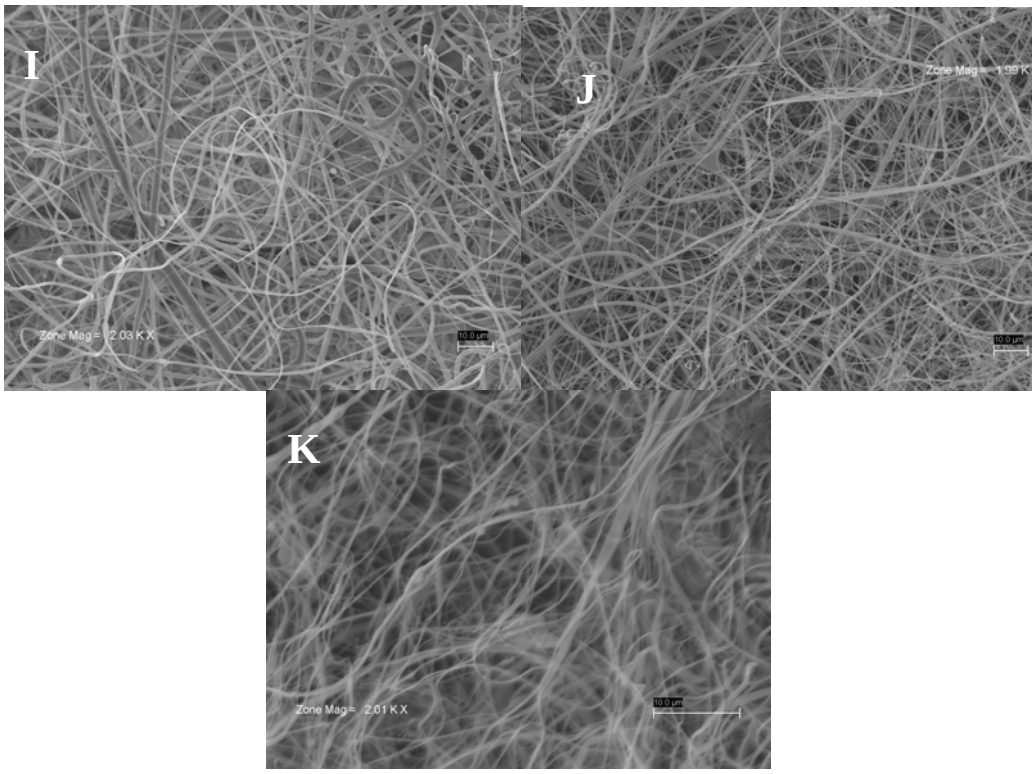

Figure 5: Figures A through K show SEM pictures taken at 2000x of dry PDO: FBG samples. Samples shown are A. 100:0, B. 90:10, C. 80:20, D. 70:30, E. 60:40, F. 50:50, G 40:60, H. 30:70, I. 20:80, J. 10:90, K. 0:100. These samples were electrospun at 4mL/hr using 4mL of total solution at a potential of 25kv.

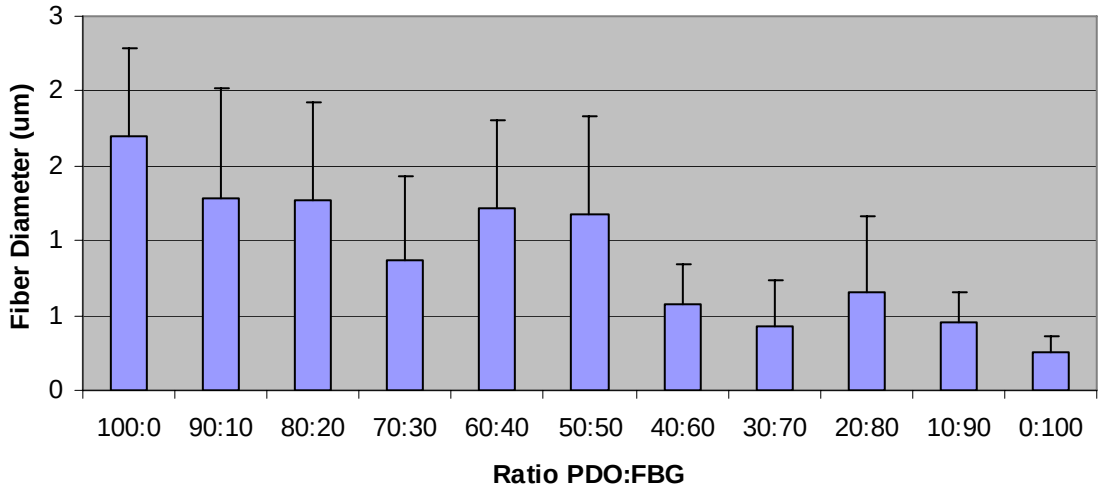

Figure 6: Relationship between PDO:FBG blends and fiber diameter.

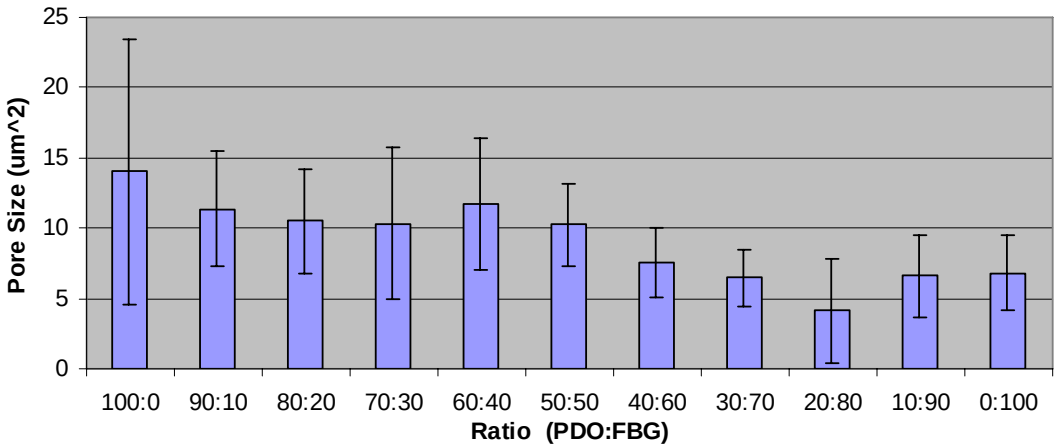

Figure 7: Average pore sizes of various rations of PDO:FBG.

Mechanical Evaluation of Electrospun Scaffolds

Modulus of elasticity calculations were performed on 11 groups, with 6 specimens from each group. The relationship between various concentrations of PDO and Fibrinogen are shown below in figure 8.

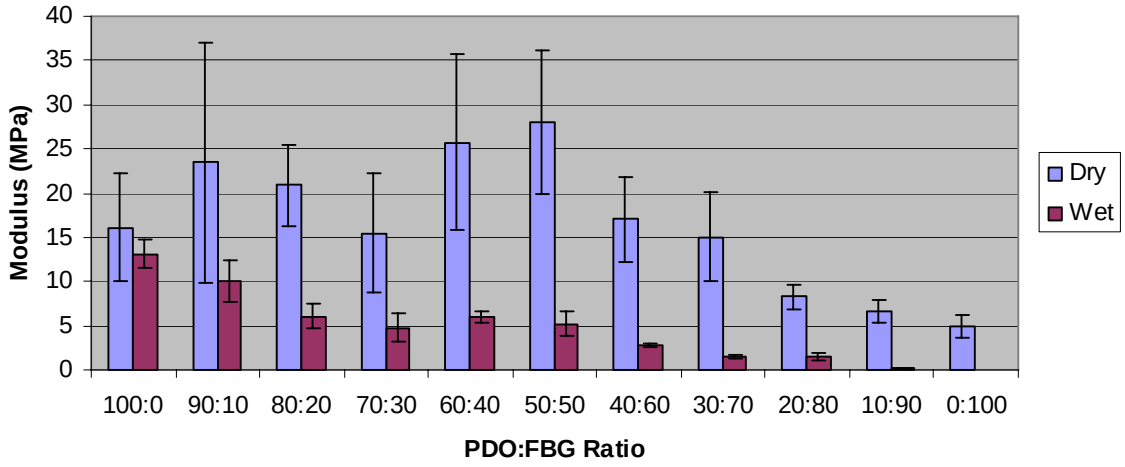

Figure 8 : Modulus of Elasticity for varying concentrations by volume of both hydrated and dry PDO:FBG blends.

Comparing dry samples of 100 PDO : 0 FBG to other samples showed significant differences between dry 50 PDO : 50 FBG samples, and dry 0 PDO : 100 FBG samples. Hydrated 100 PDO : 0 FBG differed from 30 PDO : 70 FBG, 20 PDO : 80 FBG, and 10 PDO : 90 FBG. Increasing modulus of elasticity seems to increase with increasing PDO concentrations in hydrated samples

It is interesting to note that the dry modulus of elasticity is at its peak (28.0 MPa) in 50 PDO 50 FBG samples, while the hydrated peak modulus is 13.6 MPa in 90 PDO 10 FBG samples. The lowest modulus was observed in both wet and dry samples containing higher concentrations of fibrinogen.

Peak stress was calculated from the same samples as above. Figure 9 shows the relationship between various concentrations of PDO and FBG and peak stress.
It was determined that dry 100% PDO samples were different from all samples other than 90:10 PDO:FBG samples. Hydrated samples of 100% PDO likewise differed from all other concentrations other than 90:10 PDO:FBG samples.

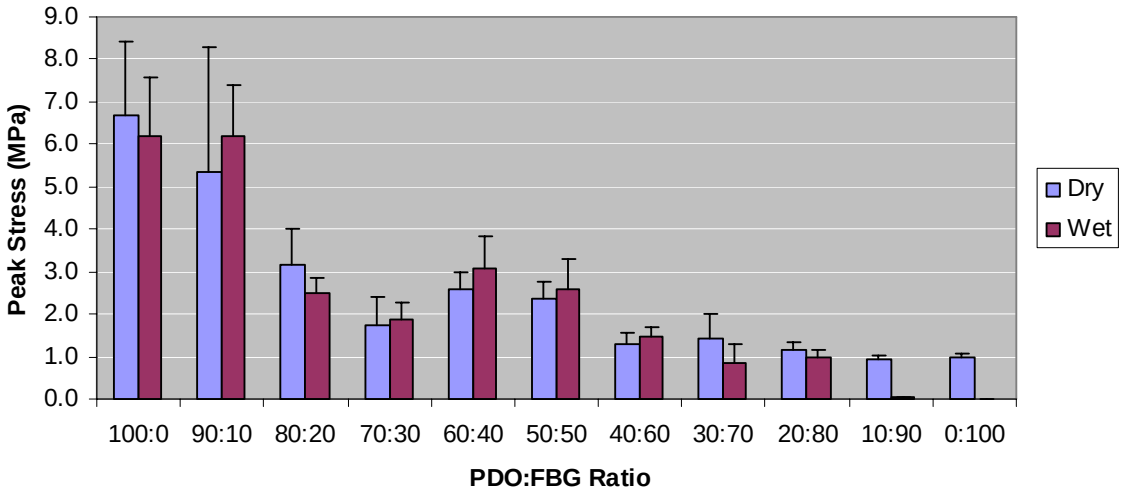

Figure 9: Graph of peak stress values for wet and hydrated ratios of PDO:FBG.

Strain at break data is shown in figure 10. Again, comparisons of strain at break at various concentrations were performed using a Tukey analysis with an *a priori* level of significance set equal to 0.05. Dry PDO samples were significantly different from all

other dry samples, while hydrated samples differed from all other samples except 10 PDO : 90 FBG samples.

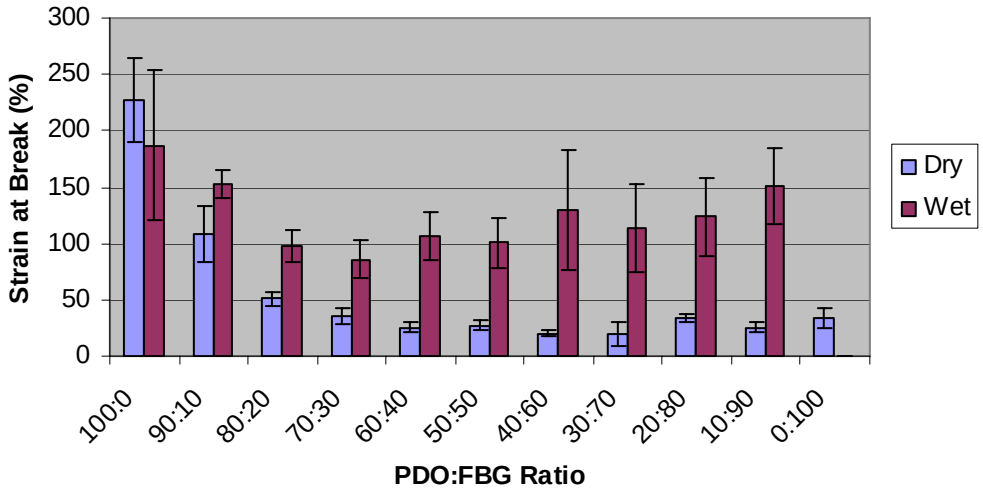

Figure 10: Relationship between concentrations of wet and hydrated PDO:FBG to strain at break.

MTS Assay

In order to quantify cells using a MTS assay, a standard curve was constructed by taking absorbance of 2500, 5000, 10000, and 20000 cell/well standards after MTS treatment. A standard curve was constructed by plotting absorbance against number of cells per well (Figure 11). A linear regression was performed, and determine to have an equation of :

$$\text{Absorbance} = 1\text{x}10^{-5} * \text{Cell Number}$$

It was determined that the linear regression had an R^2 of 0.964 , indicating a relatively good fit.

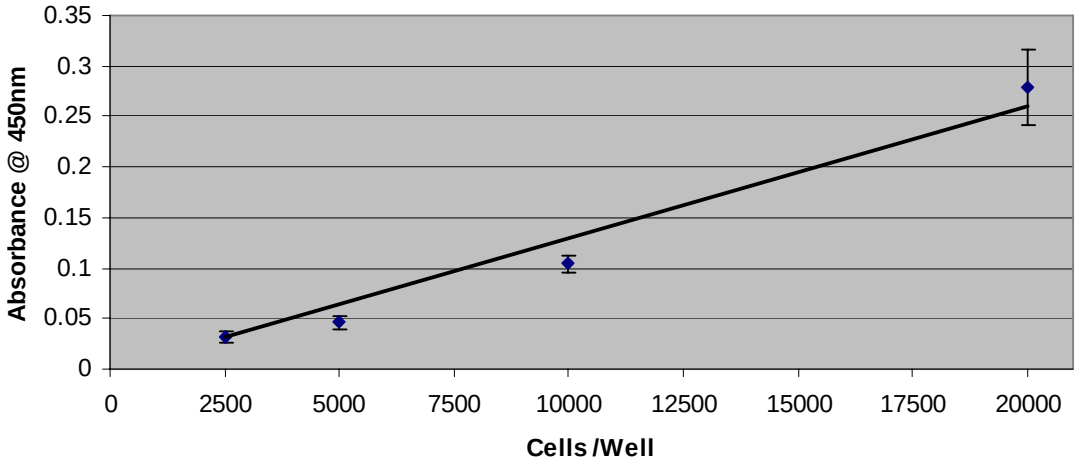

Figure 11: Relationship between absorbance at 450nm and known 2500 , 5000, 10000, and 20000 cells/well. A trend line was used to determine the relationship between absorbance and cell concentration.

One day cell cultures were assayed for proliferation using a MTS assay. The results in Figure 12 show the relationship between PDO:FBG blends and cell proliferation. Scaffolds seeded with 10,000 cells were shown to range from a minimum average of 7,300 cells on a pure PDO scaffold to a maximum average of 11,000 cells on a 90 FBG : 10 PDO scaffold. A Tukey-Kramer test was performed and no significant difference between polymer ratio and cell proliferation was observed.

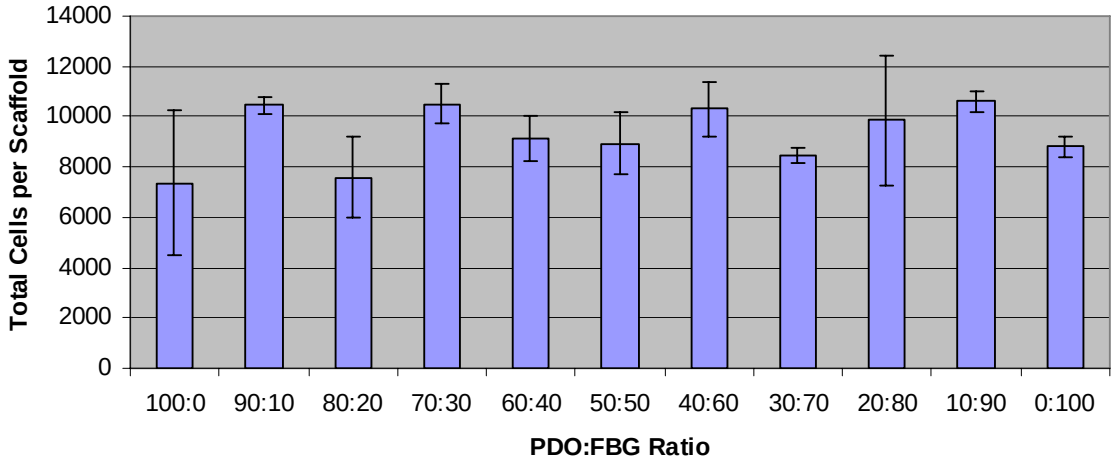

Figure 12. Relationship between cell proliferation of 10,000 cells after 1 day, and various blends of PDO:FBG determined by MTS assay.

Seven day cell cultures were assayed for proliferation in the same manner as one day cultures. The results in Figure 13 show the relationship between PDO:FBG blends and cell proliferation after 7 days. Samples of 90:10, 40:60, and 0:100 had n values of 2, 3 and 3 respectively. All other samples had an n of 5. A wide variation of values can be noted. A Tukey-Kramer test was performed, and no significant difference between polymer ratio and cell proliferation was observed.

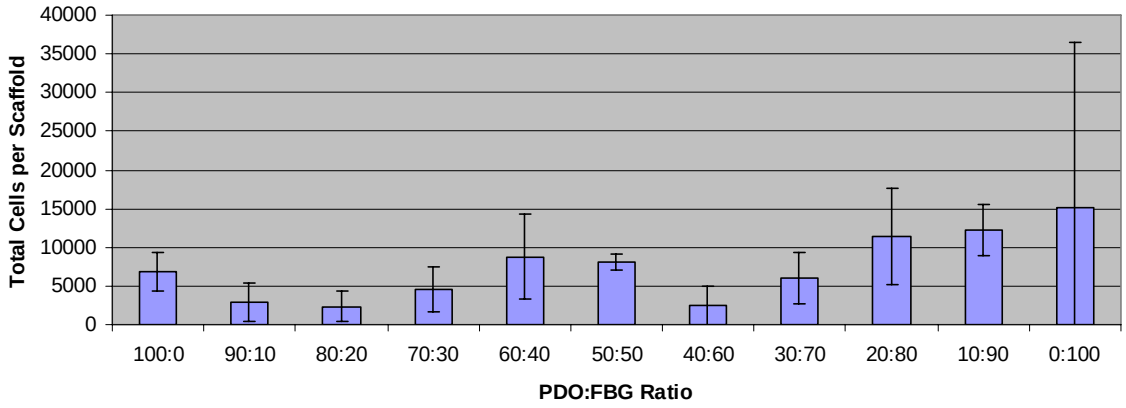

Figure 13. Relationship between cell proliferation of 10,000 cells after 7 days, and various blends of PDO:FBG determined by MTS assay.

Histology

Histological sections were taken after 1 and 7 days. Haematoxylin and Eosin (H&E) staining was used to identify cell bodies. In order to be considered a cell, an optically dense blue nuclei surrounded by a less dense region was needed for definitive identification. Samples cultured for 1 day are shown below in Figure 14. Cells on these scaffolds were scarce, and were only observed on the periphery of the scaffold. Day 7 cultures of 90:10 to 10:90 (100:0 omitted due to processing error) appeared to have an increased number of cells. Most of the cells were found on the surfaces of the scaffold, however in scaffolds containing 40:60, 20:80, and 10:90 PDO:FBG ratios cells were found to have invaded the scaffolds.

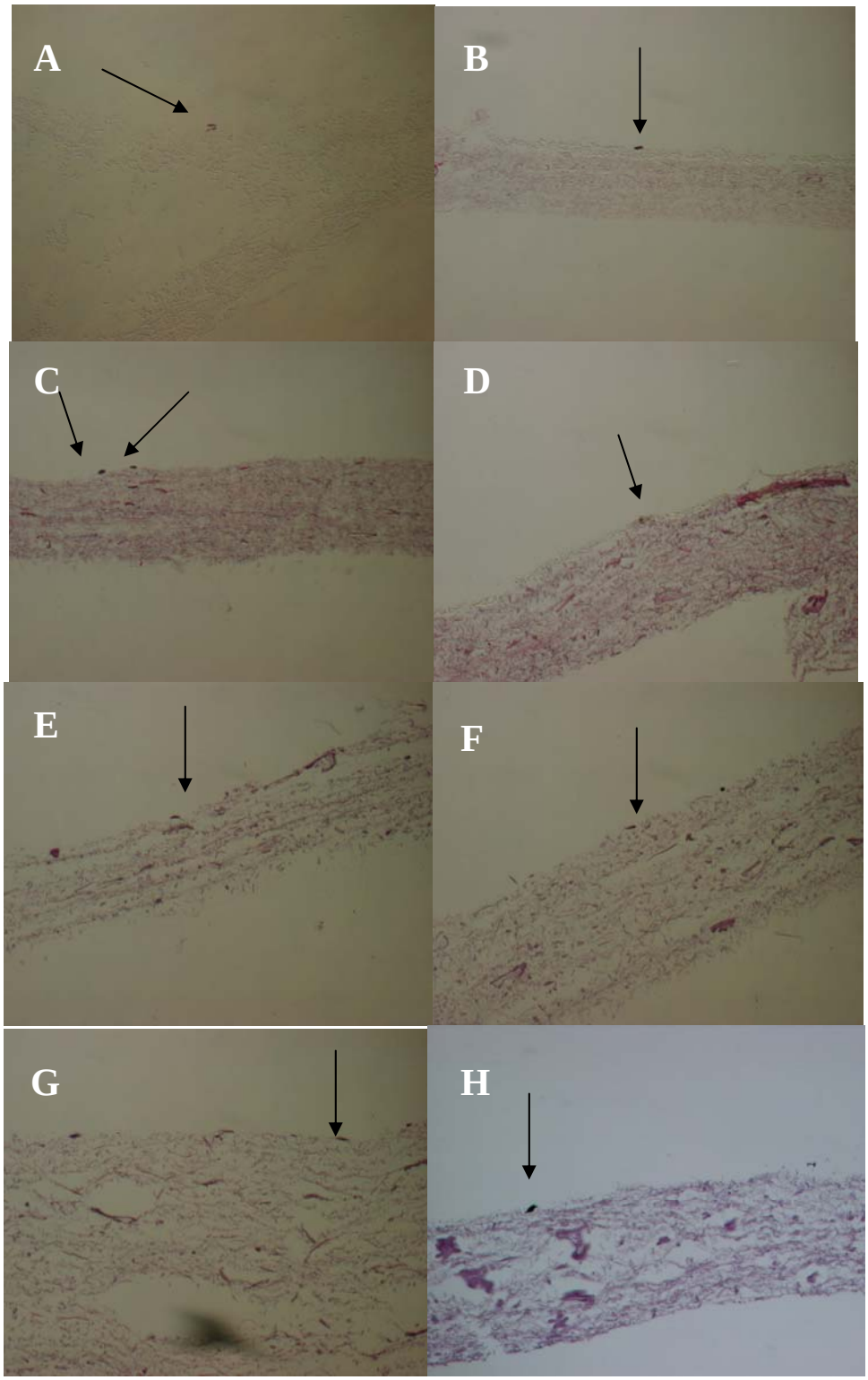

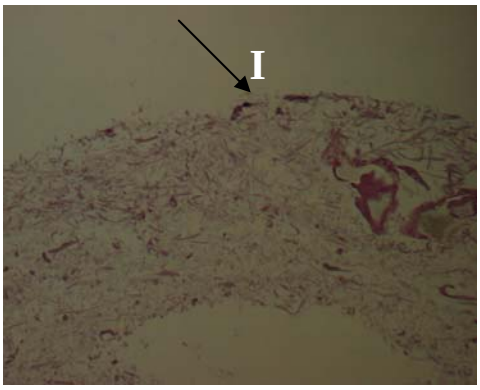

Figure 14: Figures A through I show 1 day histological sections stained with H & E staining of 100:0 to 10:90 scaffolds respectively. Samples shown are A. 100:0, B. 90:10, C. 80:20, D. 70:30, E. 60:40, F. 50:50, G 40:60, H. 30:70, I. 20:80, J. 10:90 .Scaffold were seeded with 10,000 human dermal fibroblasts. These samples were electrospun at 4mL/hr using 4mL of total solution at a potential of 25kv. Arrows indicate cells.

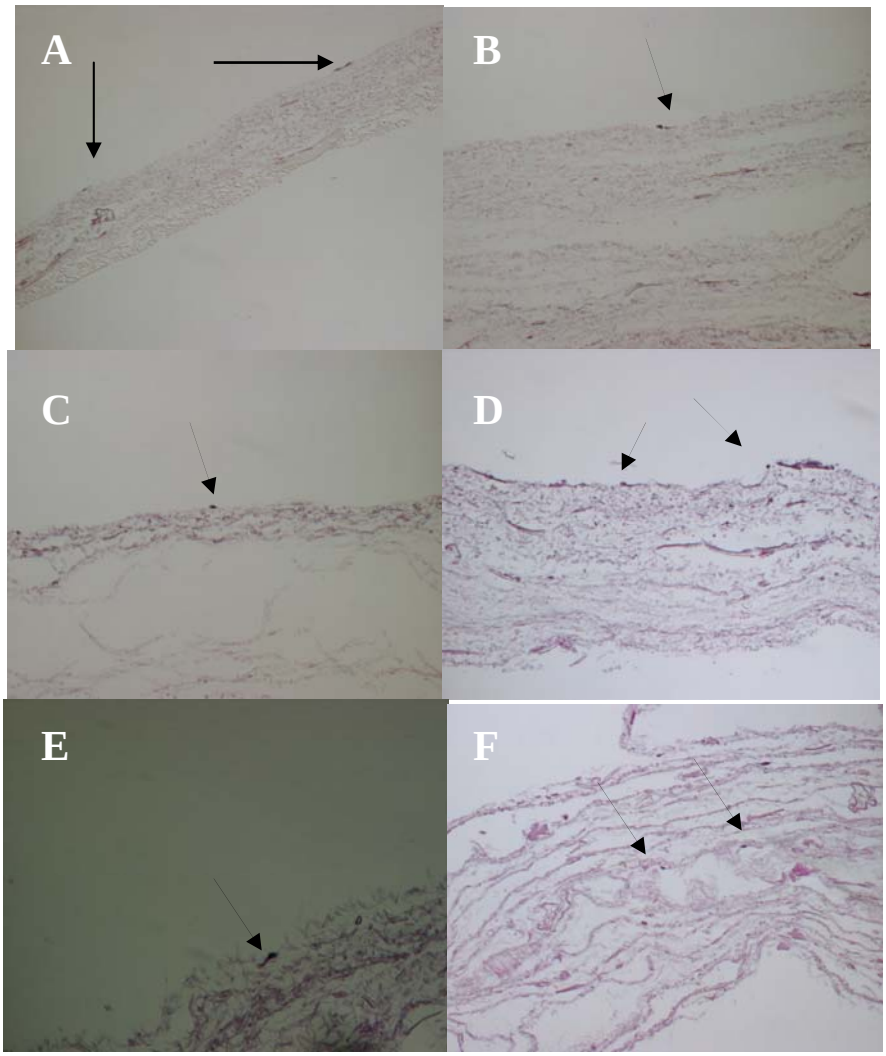

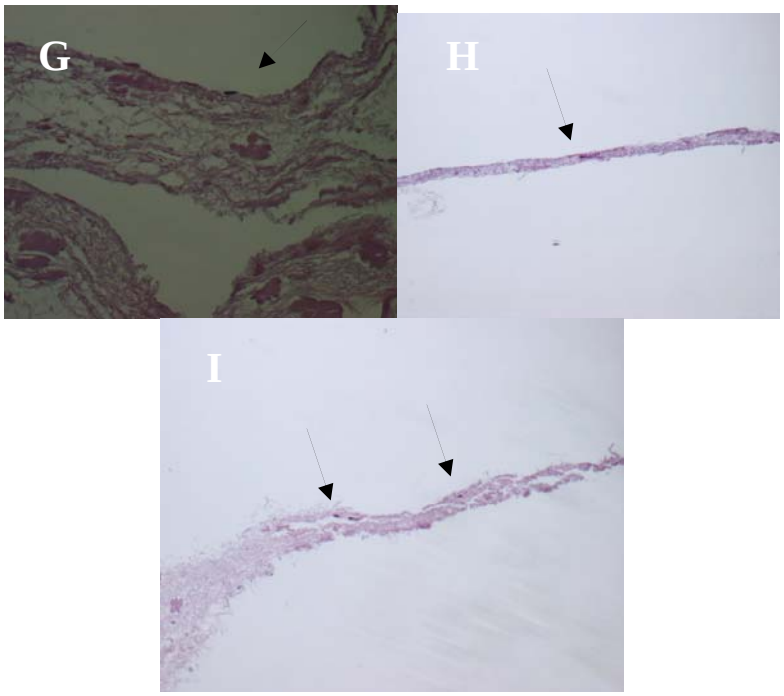

Figure 15: Figures A through I show 7 day histological sections stained with H & E staining of 90:10 to 10:90 scaffolds respectively. Samples shown are A. 90:10, B. 80:20, C. 70:30, D. 60:40, E. 50:50, F 40:60, G. 30:70, H. 20:80, I. 10:90. Scaffolds were seeded with 10,000 human dermal fibroblasts. These samples were electrospun at 4mL/hr using 4mL of total solution at a potential of 25kv. Arrows indicate cells.

Discussion

As the need for non-allographic tissue grows, so will the demand for a suitable replacement. In order to be considered, such a replacement must mimic native tissues in several ways. First, the micro and nanoscale environment of the target tissue must be mimicked in the scaffold. Specifically, scaffold fiber diameter and pore size must be similar to that of the ECM. Second, the replacement must have the mechanical strength of the target tissue. Finally, and most importantly, the scaffold must promote cell attachment and infiltration. Fulfilling these three criteria may make the scaffold more suitable for cell infiltration and proliferation. It is only when these requirements are met that the engineered scaffold might be considered as a suitable replacement.

Scaffold Characterization

The first goal of this study was to successfully electrospin synthetic PDO and naturally derived fibrinogen. Upon addition of fibrinogen to a solution containing PDO and HFP, fibrinogen precipitation occurs. Precipitation prevents successful electrospinning. Methods to blend the two polymers without precipitation of fibrinogen were investigated. Keeping solutions of PDO and fibrinogen separate until mixing at the tip of a specially machined coaxial nozzle facilitated electrospinning. SEM analysis indicated that all concentrations of PDO and FBG resulted in successful deposition of small diameter fibers on the mandrel. It was observed that only fibers were produced, and no sputtering took place.

A correlation was observed between fiber diameter and PDO:FBG ratio (Figure 8). In samples with larger than 50% ratio of PDO:FBG, average fiber diameter was similar to that of pure PDO. Samples with PDO:FBG ratios below 50% PDO had fiber diameters more closely resembling that of pure fibrinogen. It is also important to note that the average fiber diameters for each 100:0 and 0:100 ratios are similar to their previously reported literature values [37, 59]. Some fibers produced were on a scale similar to that of the native ECM. Further customization of fiber diameter can be achieved by selecting certain ratios, but all still provide acceptable diameters for tissue engineering.

Pore size was also compared to that of native tissue. Average pore size ranged from a minimum average of 6.5 μm^2 in 30:70 to a maximum average of 14.0 μm^2 in 100:0 ratios. These values all fell within the 50 nm^2 to 300 μm^2 range that has been reported to facilitate infiltration [31].

Mechanical Characterization

Polydioxanone has been reported to demonstrate strong mechanical characteristic, even after electrospinning [37]. This work intends to preserve the characteristics in all scaffold ratios. A trend in hydrated samples exists between PDO content and modulus. Higher PDO content increased elastic modulus. Samples with predominately PDO fibers, will maintain the characteristics of pure PDO. Hydrated blends ultimately mimic the scaffold in its target environment, therefore trends in hydrated samples are more pertinent to this study.

Strain at break was significantly larger in 100:0 and 90:10 for both dry and hydrated samples. These samples, containing mostly PDO, exhibited stain at break properties closely associated to pure electrospun PDO. All hydrated samples containing fibrinogen had higher strain at break than their dry counterparts.

Peak stress of 100:0 and 90:10 dry and hydrated samples was significantly different compared to those of the other samples. Any further decrease of PDO or increase in fibrinogen after this point yields a significantly diminished peak stress. Although peak stress decreases, both dry and wet samples with PDO:FBG ratios above 10:90 exhibited superior peak stress values compared to 0.2 MPa reported for human ureter[61]. The roughly ten-fold increase in peak stress values is significant. It is important that the scaffold retain sufficient stress values as remodeling and degradation take place.

Mechanical testing of these scaffolds served to elucidate the effect of incorporation of fibrinogen into polydioxnaone scaffolds. Inclusion of fibrinogen significantly altered mechanical properties compared to those of pure PDO. Fibrinogen incorporation did not alter the scaffolds to the point where they were made weak. In fact, samples with ratios of PDO:FBG over 10:90 proved mechanically superior to that of the human ureter. It is important to note that scaffolds containing pure fibrinogen did not have enough structural integrity to allow for mechanical testing after hydration.

Cell Proliferation Assays

The results of the one day MTS assay indicated that roughly the same number of seeded cells remained viable on the scaffold after one day. Surprisingly, the seven day

assay showed a high degree of variability with several samples showing lower than expected cell counts. Although it is difficult to draw finite conclusions, data from 20:80, 10:90, and 0:100 samples on average demonstrated a slight increase in average number of cells despite a high degree of variability.

It is suspected that both the variability and low cell counts are due to the nature of the scaffold and MTS assay. The MTS assay involves the conversion of MTS reagent to soluble formazan dye, which absorbs light around 450nm. Not only must the MTS reagent penetrate into the scaffold, but once converted to formazan, it must be homogenously redistributed throughout the culture media. Although samples were agitated prior to testing, complete redistribution of formazan may not have occurred. In addition, it is possible that the dye simply become bound and stuck to some of the scaffolds. Based on this contention, it is suggested that future studies involve altered protocols, or alternatives to the MTS assay.

Histology

H & E staining was performed on 1 and 7 day samples. After culture for one day, all ratios of PDO:FBG showed fibroblasts on their surface. Immediate infiltration was not assumed, and we hypothesized that cells would be attached to the surface of the scaffolds. We also hypothesized that over a seven day incubation, cells would migrate through the thickness of the scaffold. PDO:FBG ratios of 40:60, 20:80, and 10:90 all were found to have cells that infiltrated, while other scaffolds had cells on their surface. It is interesting to

note that scaffolds in which infiltration occurred all had larger amounts of fibrinogen than PDO. Therefore a threshold ratio might exist that promotes infiltration.

Conclusions

The goals of this study were to blend two previously electrospun polymers, PDO and fibrinogen and to produce a blended product that retained both the mechanical strength of PDO and the cell growth promoting characteristics of pure fibrinogen. The incorporation of PDO with fibrinogen increased the overall mechanical strength compared to the strength of only fibrinogen. Additionally, fiber diameter and pore size were characterized. Fiber diameter and pore size values remained within limits compared to reported values of the ECM. The ability of these scaffolds to facilitate attachment and proliferation was determined with an MTS assay and observed qualitatively through histological staining. Both assessments showed that scaffolds supported cell growth. Histological staining showed three ratios of PDO:FBG that facilitated cell infiltration. These three ratios of PDO:FBG, 40:60 , 20:80, and 10:90, all supported cell infiltration after a 7 day culture.

The applications of a scaffold that is both bioactive and structurally similar to native tissue are numerous. Specifically, these scaffolds were intended for use in urological applications. Ureter and urethral stricture, due to obstruction or congenital abnormalities respectively, are pervasive. Current treatments are not sufficient, and the development of a new tissue scaffold might aide future work.

Although this study successfully indicated cell infiltration into blended scaffolds, it is not without flaw. The MTS assay proved imprecise with 7 day culture samples. Cell infiltration into the scaffold was assumed, and penetration of MTS reagent may have been

impeded by the scaffold itself. We also suspected that upon shipping samples for histology, some detachment of cells may occur.

Future work must be conducted in order to prove further the effectiveness of scaffolds made from PDO and fibrinogen. Smooth muscle cells, and epithelial cells of the ureter and urethra must be used to determine their proliferation and infiltration into these scaffolds. Longer term studies of the degradation of these scaffolds must also be conducted. We have hypothesized that cleaving fibrinogen to fibrin via thrombin might expose more bioactive domains. Crosslinking fibrin via factor XIII might also serve to benefit cellular response. Finally, the effectiveness of these scaffolds *in vivo* must be considered.

Literature Cited

1. Langer, R. and J.P. Vacanti, *Tissue Engineering.* Science, 1993. **260**(5110): p. 920-926.
2. Schulak, J.A., *What's new in general surgery: Transplantation.* Journal of the American College of Surgeons, 2005. **200**(3): p. 409-417.
3. Simpson, D.G., *Dermal templates and the wound-healing paradigm: the promise of tissue regeneration.* Expert Review of Medical Devices, 2006. **3**(4): p. 471-484.
4. Despopoulos, A.S., Stefan *Color Atlas of Physiology*. 5th ed. 2003, Stuttgart, Germany: Georg Thieme Verlag.
5. Klahr, S., *Urinary Tract Obstruction*, in *Diseases of the Kidney and Urinary Tract*, R.W. Schrier, Editor. 2001, Lippincott Williams & Wilkins. p. 473.
6. Fontaine, E., et al., *Twenty-year experience with jejunal conduits.* Urology, 1997. **50**(2): p. 207-213.
7. Hautmann, R.E., *Urinary diversion: Ileal conduit to neobladder.* Journal of Urology, 2003. **169**(3): p. 834-842.
8. Palmer, J.M., F.G. Zweiman, and Assaykee.Ta, *Renal Hypertension Due to Hydronephrosis with Normal Plasma Renin Activity.* New England Journal of Medicine, 1970. **283**(19): p. 1032-&.
9. Sakamoto, N., et al., *Recurrence of Bladder-Tumors Following Surgery for Transitional Cell-Carcinoma of the Upper Urinary-Tract.* European Urology, 1991. **20**(2): p. 136-139.
10. Atala, A., *Congenital Urological Anomalies*, in *Diseases of the Kidney and Urinary Tract*, R.W. Schrier, Editor. 2001, Lippincott Williams & Wilkins. p. 415.
11. Shenfeld, O.Z., et al., *Urethral reconstruction for patients with a history of hypospadias repair.* Journal of Urology, 2007. **177**(4): p. 38-38.
12. Barbagli, G. and M. Lazzeri, *Urethral reconstruction.* Current Opinion in Urology, 2006. **16**(6): p. 391-395.

13. Milroy, E., *Stents in urethral stricture repair.* Urologe-Ausgabe A, 1998. **37**(1): p. 51-55.
14. Whitson, J.M., et al., *Long term efficacy of penile fasciocutaneous flaps for the treatment of anterior urethral stricture disease.* Journal of Urology, 2007. **177**(4): p. 37-38.
15. Hauser, S., et al., *Small intestine submucosa in urethral stricture repair in a consecutive series.* Urology, 2006. **68**(2): p. 263-266.
16. Tsivian, A., S. Benjamin, and A.A. Sidi, *Ventral buccal mucosal onlay graft urethroplasty for penile urethral stricture.* Journal of Urology, 2007. **177**(4): p. 160-161.
17. Tanagho, E.A., *Case against Incorporation of Bowel Segments into Closed Urinary System.* Journal of Urology, 1975. **113**(6): p. 796-802.
18. Bazeed, M.A., et al., *Ileal Replacement of the Bilharzial Ureter - Is It Worthwhile.* Journal of Urology, 1983. **130**(2): p. 245-248.
19. Ubrig, B. and S. Roth, *Reconfigured colon segments as a ureteral substitute.* World Journal of Urology, 2003. **21**(3): p. 119-122.
20. Chen, F., J.J. Yoo, and A. Atala, *Acellular collagen matrix as a possible "off the shelf" biomaterial for urethral repair.* Urology, 1999. **54**(3): p. 407-410.
21. Barbalias, G.A., et al., *Ureteroileal anastomotic strictures: An innovative approach with metallic stents.* Journal of Urology, 1998. **160**(4): p. 1270-1273.
22. Leveillee, R.J., et al., *A new self-expanding lined stent-graft in the dog ureter: Radiological, gross, histopathological and scanning electron microscopic findings.* Journal of Urology, 1998. **160**(5): p. 1877-1882.
23. Tachibana, M., G.R. Nagamatsu, and J.C. Addonizio, *Ureteral Replacement Using Collagen Sponge Tube Grafts.* Journal of Urology, 1985. **133**(5): p. 866-869.
24. Atala, A., et al., *Formation of Urothelial Structures Invivo from Dissociated Cells Attached to Biodegradable Polymer Scaffolds Invitro.* Journal of Urology, 1992. **148**(2): p. 658-662.
25. Shokeir, A., et al., *Acellular matrix tube for canine urethral replacement: Is it fact or fiction?* Journal of Urology, 2004. **171**(1): p. 453-456.
26. Park, J.E., G.A. Keller, and N. Ferrara, *Vascular Endothelial Growth-Factor (Vegf) Isoforms - Differential Deposition into the Subepithelial Extracellular-Matrix and Bioactivity of Extracellular Matrix-Bound Vegf.* Molecular Biology of the Cell, 1993. **4**(12): p. 1317-1326.
27. Boudriot, U., et al., *Electrospinning approaches toward scaffold engineering - A brief overview.* Artificial Organs, 2006. **30**(10): p. 785-792.
28. Martins-Green, M., *Dynamics of Cell-ECM Interactions*, in *Principles of Tissue Engineering* R.P.L. Lanza, Robert , Vacanti, Joseph, Editor. 2000Academic Press. p. 33-55.
29. Giancotti, F.G. and E. Ruoslahti, *Transduction - Integrin signaling.* Science, 1999. **285**(5430): p. 1028-1032.
30. Smith, L.A. and P.X. Ma, *Nano-fibrous scaffolds for tissue engineering.* Colloids and Surfaces B-Biointerfaces, 2004. **39**(3): p. 125-131.

31. Levesque, S.G., R.M. Lim, and M.S. Shoichet, *Macroporous interconnected dextran scaffolds of controlled porosity for tissue-engineering applications.* Biomaterials, 2005. **26**(35): p. 7436-7446.
32. Telemeco, T.A., et al., *Regulation of cellular infiltration into tissue engineering scaffolds composed of submicron diameter fibrils produced by electrospinning.* Acta Biomaterialia, 2005. **1**(4): p. 377-385.
33. Zeleny, J., *Instability of Electrified Liquid Surfaces.* Physical Review, 1917. **10**: p. 1-6.
34. Huang, Z.M., et al., *A review on polymer nanofibers by electrospinning and their applications in nanocomposites.* Composites Science and Technology, 2003. **63**(15): p. 2223-2253.
35. Frenot, A. and I.S. Chronakis, *Polymer nanofibers assembled by electrospinning.* Current Opinion in Colloid & Interface Science, 2003. **8**(1): p. 64-75.
36. Kricheldorf, H.R. and D.O. Damrau, *Polylactones, 42 - Zn L-lactate-catalyzed polymerizations of 1,4-dioxan-2-one.* Macromolecular Chemistry and Physics, 1998. **199**(6): p. 1089-1097.
37. Boland, E.D., et al., *Electrospinning polydioxanone for biomedical applications.* Acta Biomaterialia, 2005. **1**(1): p. 115-123.
38. Molea, G., et al., *Comparative study on biocompatibility and absorption times of three absorbable monofilament suture materials (Polydioxanone, Poliglecaprone 25, Glycomer 631).* British Journal of Plastic Surgery, 2000. **53**(2): p. 137-141.
39. Wainstein, M., J. Anderson, and J.S. Elder, *Comparison of effects of suture materials on wound healing in a rabbit pyeloplasty model.* Urology, 1997. **49**(2): p. 261-264.
40. Cady, R.B., et al., *Physeal response to absorbable polydioxanone bone pins in growing rabbits.* Journal of Biomedical Materials Research, 1999. **48**(3): p. 211-215.
41. Kontio, R., et al., *Effectiveness of operative treatment of internal orbital wall fracture with polydioxanone implant.* International Journal of Oral and Maxillofacial Surgery, 2001. **30**(4): p. 278-285.
42. Herrick, S., et al., *Fibrinogen.* International Journal of Biochemistry & Cell Biology, 1999. **31**(7): p. 741-746.
43. Rand, M.L.M., Robert : , *Hemostasis & Thrombosis*, in *Harper's Illustrated Biochemistry*R.K.G. Murray, Daryl K; Mayes,Peter A., Editor. 2000.
44. Berg, J.T., John; Stryer, Lubert, *Regulatory Strategies: Enzymes and Hemoglobin*, in *Biochemistry*. 2002.
45. Murray, R.K., et al., *Plasma Proteins & Immunoglobulins*, in *Harper's Illustrated Biochemistry*, R.K. Murray, Editor. 2004. p. 599.
46. Rooney, M.M., et al., *The contribution of the three hypothesized integrin-binding sites in fibrinogen to platelet-mediated clot retraction.* Blood, 1998. **92**(7): p. 2374-2381.
47. Sporn, L.A., L.A. Bunce, and C.W. Francis, *Cell-Proliferation on Fibrin - Modulation by Fibrinopeptide Cleavage.* Blood, 1995. **86**(5): p. 1802-1810.

48. Heron, A., et al., *Mitogenic effect of fibrinogen on hematopoietic cells: Involvement of two distinct specific receptors, MFR and ICAM-1.* Biochemical and Biophysical Research Communications, 1998. **246**(1): p. 231-237.
49. Gray, A.J., et al., *The Mitogenic Effects of the B-Beta Chain of Fibrinogen Are Mediated through Cell-Surface Calreticulin.* Journal of Biological Chemistry, 1995. **270**(44): p. 26602-26606.
50. Skogen, W.F., et al., *Fibrinogen-Derived Peptide B-Beta-1-42 Is a Multidomained Neutrophil Chemoattractant.* Blood, 1988. **71**(5): p. 1475-1479.
51. Underwood, S., et al., *Wet extrusion of fibronectin-fibrinogen cables for application in tissue engineering.* Biotechnology and Bioengineering, 2001. **73**(4): p. 295-305.
52. Peretti, G.M., et al., *A biomechanical analysis of an engineered cell-scaffold implant for cartilage repair.* Annals of Plastic Surgery, 2001. **46**(5): p. 533-537.
53. Passaretti, D., et al., *Cultured chondrocytes produce injectable tissue-engineered cartilage in hydrogel polymer.* Tissue Engineering, 2001. **7**(6): p. 805-815.
54. Ahmed, Z., S. Underwood, and R.A. Brown, *Low concentrations of fibrinogen increase cell migration speed on fibronectin/fibrinogen composite cables.* Cell Motility and the Cytoskeleton, 2000. **46**(1): p. 6-16.
55. Seliktar, D., *Extracellular Stimulation in Tissue Engineering.* New York Academy of Science, 2005. **1047**: p. 386-395.
56. Reneker, D.H. and I. Chun, *Nanometre diameter fibres of polymer, produced by electrospinning.* Nanotechnology, 1996. **7**(3): p. 216-223.
57. Doshi, J. and D.H. Reneker, *Electrospinning Process and Applications of Electrospun Fibers.* Journal of Electrostatics, 1995. **35**(2-3): p. 151-160.
58. Wnek, G.E.C., Marcus E.; Simpson, David G.; Bowling, Gary L. , *Electrospinning of Nanofiber Fibrinogen Structures.* Nano Letters, 2003. **3**(2): p. 213-216.
59. McManus, M.C., et al., *Mechanical properties of electrospun fibrinogen structures.* Acta Biomaterialia, 2006. **2**(1): p. 19-28.
60. Clark, R.A.F., et al., *Fibronectin and Fibrin Provide a Provisional Matrix for Epidermal-Cell Migration During Wound Reepithelialization.* Journal of Investigative Dermatology, 1982. **79**(5): p. 264-269.
61. Yamada, H., *Strength of biological materials*, ed. G. Evans. 1973. 209.

APPENDIX A

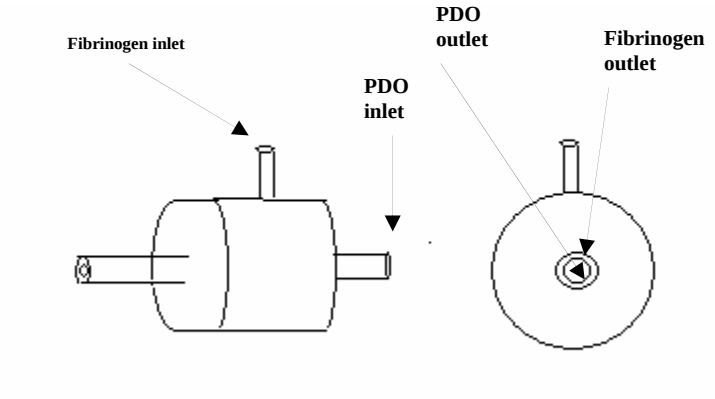

Coaxial Electrospinning Nozzle. Left figure shows the side view of the nozzle. The two labeled inlets are for PDO and fibrinogen. The right figure shows the coaxial outlet of the nozzle.

APPENDIX B

	100:0	80:20	90:10	60:40	50:50	70:30	20:80	40:60	10:90	30:70	0:100
100:0		*	*	*	*	*	*	*	*	*	*
80:20	*					*	*	*	*	*	*
90:10	*					*	*	*	*	*	*
60:40	*					*	*	*	*	*	*
50:50	*						*	*	*	*	*
70:30	*		*	*				*	*	*	*
20:80	*	*	*	*	*						*
40:60	*	*	*	*	*	*					*
10:90	*	*	*	*	*	*					
30:70	*	*	*	*	*	*					
0:100	*	*	*	*	*	*	*	*			

Table of statistical differences between fiber diameter and PDO:FBG ratios. Diameters were determined using ImageTool. Asterisks (*) indicate significant difference.

	100:0	60:40	90:10	80:20	70:30	50:50	40:60	0:100	10:90	30:70	20:80
100:0		*	*	*	*	*	*	*	*	*	*
60:40			*	*	*	*	*	*	*	*	*
90:10				*	*	*	*	*	*	*	*
80:20					*	*	*	*	*	*	*
70:30						*	*	*	*	*	*
50:50							*	*	*	*	*
40:60								*	*	*	*
0:100									*	*	*
10:90										*	*
30:70											*
20:80											

Table of statistical difference between pore size and PDO:FBG rations. Pore size was determined using ImageTool. Asterisks indicate significant difference.

	100:0 dry	90:10 wet	100:0 wet	90:10 dry	80:20 Dry	60:40 Wet	50:50 Wet	60:40 Dry	80:20 Wet	50:50 Dry	70:30 Wet	70:30 Dry	40:60 Wet	30:70 Wet	40:60 Dry	20:80 Dry	0:100 Dry	20:80 Dry	10:90 Wet	30:70 Wet
100:0 Dry					*	*	*	*	*	*	*	*	*	*	*	*	*	*	*	*
90:10 Wet					*	*	*	*	*	*	*	*	*	*	*	*	*	*	*	*
100:0 wet					*	*	*	*	*	*	*	*	*	*	*	*	*	*	*	*

.

Table of statistical difference between preak stress and PDO:FBG rations. Peak stress was determined using a MTS Bionix 200 tensile tester. Asterisks indicate significant difference.

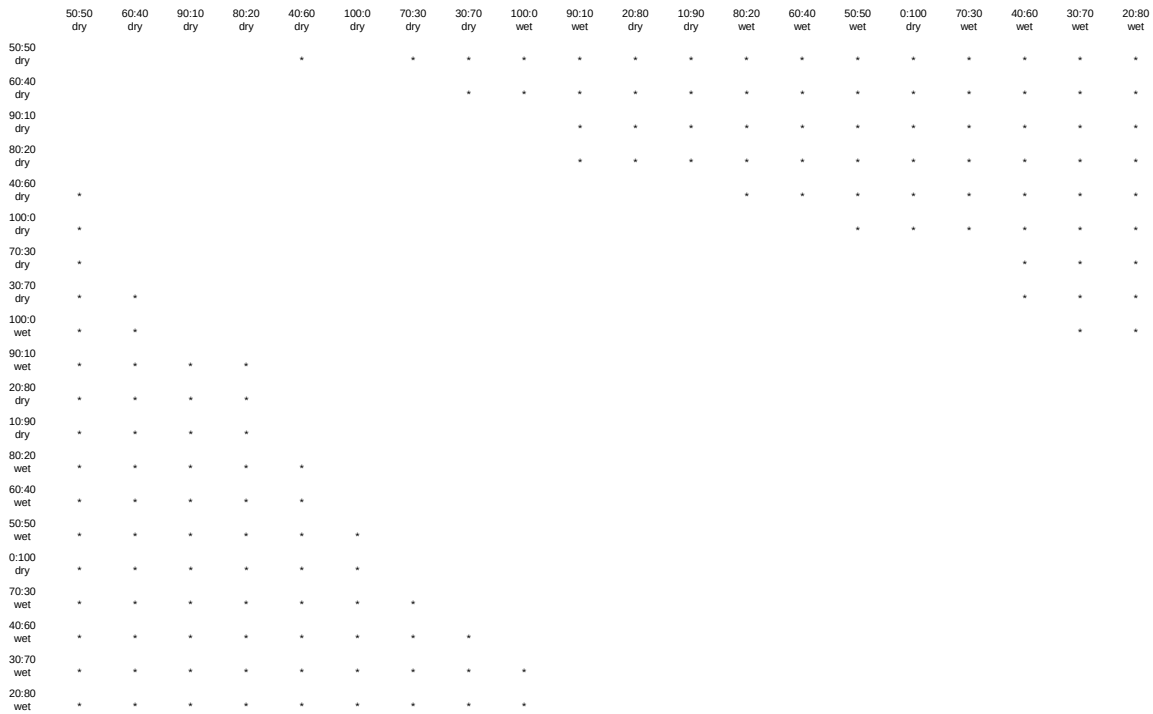

10:90 wet	* * * * * * * * *

Table of statistical difference between elastic modulus and PDO:FBG rations. Peak stress was determined using a MTS Bionix 200 tensile tester. Asterisks indicate significant difference.

	100:0 Dry	100:0 Wet	90:10 wet	10:90 wet	40:60 wet	20:80 wet	30:70 wet	90:10 dry	60:40 wet	50:50 Wet	80:20 dry	70:30 wet	80:20 dry	70:30 dru	20:80 dry	0:100 dry	50:50 dry	60:40 dry	10:90 dry	40:60 dry
100:0 Dry			*	*	*	*	*	*	*	*	*	*	*	*	*	*	*	*	*	*
100:0 Wet					*	*	*	*	*	*	*	*	*	*	*	*	*	*	*	*
90:10 wet	*											*	*	*	*	*	*	*	*	*
10:90 wet	*	*										*	*	*	*	*	*	*	*	*
40:60 wet	*	*											*	*	*	*	*	*	*	*
20:80 wet	*	*											*	*	*	*	*	*	*	*
30:70 wet	*	*											*	*	*	*	*	*	*	*
90:10 dry	*	*											*	*	*	*	*	*	*	*
60:40 wet	*	*												*	*	*	*	*	*	*
50:50 wet	*	*												*	*	*	*	*	*	*
80:20 dry	*	*												*	*	*	*	*	*	*
70:30 wet	*	*	*	*													*	*	*	*
80:20 dry	*	*	*	*	*	*	*	*												
70:30 dru	*	*	*	*	*	*	*	*	*	*	*									
20:80 dry	*	*	*	*	*	*	*	*	*	*	*									
0:100 dry	*	*	*	*	*	*	*	*	*	*	*									
50:50 dry	*	*	*	*	*	*	*	*	*	*	*	*								
60:40 dry	*	*	*	*	*	*	*	*	*	*	*	*								
10:90 dry	*	*	*	*	*	*	*	*	*	*	*	*								
40:60 dry	*	*	*	*	*	*	*	*	*	*	*	*								
30:70 dry	*	*	*	*	*	*	*	*	*	*	*	*								

Table of statistical difference between elastic modulus and PDO:FBG rations. Peak stress was determined using a MTS Bionix 200 tensile tester. Asterisks indicate significant difference.

VITA

` Joshua Grant was born on September 12th, 1982 in West Palm Beach, Florida. He attended Saint Andrews High School, from which he graduated in 2001. He moved to Baltimore, MD in 2001 and attended Goucher College where he received a Bachelor in Arts degree in Chemistry in 2005. In 2005, he moved to Richmond, Virginia where he enrolled in graduate studies in Physiology. He received his Masters of Science in Physiology in the spring of 2007. He plans to attend Lake Erie College of Osteopathic Medicine, in Bradenton, Florida in the fall of 2007.